# MULTISPECTRAL IMAGING FOR ANALYZING ANCIENT MANUSCRIPTS

*Martin Lettner and Robert Sablatnig*

Pattern Recognition and Image Processing Group
Institute of Computer Aided Automation, Vienna University of Technology
1040, Vienna, Austria
phone: + 43 (0)1 58801 18353, fax: + 43 (0) 58801 18392 , email: lettner@prip.tuwien.ac.at
web: www.prip.tuwien.ac.at/lettner

## ABSTRACT

In this paper we propose a method for segmenting characters in multispectral images of ancient documents. Due to the low quality of the document images the main idea of our study is to combine the multispectral behavior and contextual spatial information. Therefore we utilize a Markov Random Field model using the spectral information of the images and stroke properties to include spatial dependencies of the characters. The whole process is parameter free since we calculate the stroke properties and the Gaussian parameters for the imaging model automatically. The study shows the effectiveness of using multispectral data for a computer aided analysis of ancient text documents. We compare the results of the proposed segmentation method to traditional methods based on color images as well as gray level images.

## 1. INTRODUCTION

Multispectral imaging offers a technique for the analysis and preservation of ancient documents. The main advantage in analyzing different spectral ranges extending also the visible light is the additional information which cannot be seen by the human eye [14]. Thus it offers the possibility of handling palimpsests[1] or damaging caused by age [6, 14]. Recent studies in multispectral imaging for historical manuscripts focused particularly on the revisualization of the underwritten (erased) text in palimpsests where methods like the Independent Component Analysis [15] or the Principal Component Analysis [6, 14] are applied. Others are interested in a general enhancement of the readability independent of underwritten or overwritten text [9]. In order to prepare digital documents for further computer aided analysis and to enable the use of simplified analysis techniques, e.g. feature extraction or Optical Character Recognition (OCR), usually binary images are produced.

This paper is concerned with the segmentation of characters in MultiSpectral Images (MSI) from ancient manuscripts. The challenges we have to deal with are caused by the documents age and include non-uniform appearance of the writing and the background, blur of the background, fading out of the ink and poor contrast, mold, water stains or humidity.

While traditional character segmentation methods for color or MSI consider the color or spectral component [10] the main idea of our approach is to improve the segmentation accuracy by including contextual information in terms of pixel relations. Therefore we utilize the multispectral behavior of the MSI and combine spatial and spectral features. Recent studies exploit the combination of spectral and spatial components but treat spectral and spatial components successively. Mancas-Thillou et al. use color clustering and subsequently a Gabor-based filter to combine color with spatial information but the method is not able to handle poor contrast images [19]. Wang et al. combines edge information, watershed transformation and clustering for character segmentation in color images [20].

In contrast to previous studies we arrange the combination of spatial and spectral components in a straightforward way. Therefore, we utilize a Markov Random Field (MRF) model which provides a probability theory for analyzing spatial or contextual dependencies [11]. Applications in computer vision like color image segmentation [8], stereo matching or image denoising [7] can be elegantly expressed as MRFs [18] which have been also adopted for document image analysis of panchromatic images. For instance, Wolf and Doerman use MRF models for the binarization of low quality text [21]. Their model for the spatial relationship is defined on a neighborhood of $4 \times 4$ pixel cliques. Cao and Govindarayu use MRFs for the binarization of degraded handwritten forms [3] where the spatial relations are obtained from a training set of high quality binarized images and consist of 114 representatives of shared patches.

Since there is no high quality text available for generating patches we propose to incorporate stroke characteristics to cover the spatial or contextual dependencies of characters. We tested the proposed method on MSI of an ancient Slavonic missal written on parchment. The results are compared to conventional color segmentation methods and to binarization methods applied on selected single band images.

This paper is organized as follows. Section 2 introduces the multispectral images and the camera system used for the acquisition process. Section 3 explains the preprocessing of the images and Section 4 introduces the MRF based segmentation methodology. Experiments and results are presented in Section 5 and Section 6 finishes the paper with a conclusion and an outlook.

## 2. MSI IMAGES OF ANCIENT DOCUMENTS

Multispectral imaging applied in the spectral range from Ultra Violet (UV), VISible light range (VIS) up to the Near InfraRed (NIR) range combines conventional imaging and spectrometry to acquire both spatial and spectral information from an object. The acquisition setup used for the missal consists of a digital color camera and a scientific NIR camera. Color images and UV fluorescence images are captured with a Nikon RGB camera providing a resolution of $4288 \times 2848$ pixels. These images are particularly dedicated

[1] A palimpsest is a parchment which was rewritten after the first text has been erased.

for visualization purposes. For the MSI we use a Hamamatsu C9300-124 camera with a spectral sensitivity from UV to NIR (330nm - 1000nm) and a resolution of $4000 \times 2672$ pixels. A filter wheel mounted in front of the camera selects different spectral images. Figure 3 shows the alignment of the two cameras. The setup leads to a spatial resolution of 565 dpi for the MSI and a resolution of approximately 500 dpi for the conventional color camera. Since every folio is captured with both cameras, a shift of the page between the cameras is necessary. Due to the use of optical filters [2] an image registration process is applied which is described in [4].

For the MSI we use four band-pass filters with a peak of 450nm (blue), 550nm (green), 650nm (red), 780nm (NIR), two long-pass filters with a cut-off frequency of 400nm (UV fluorescence) and 800nm (IR reflectography), and a short-pass filter with a cut-off frequency of 400nm to capture UV reflectography images. Using different illumination we obtain nine different spectral images. The filters are summarized in Table 1 and their spectral transmittance is visualized in Figure 1 on the left hand side.

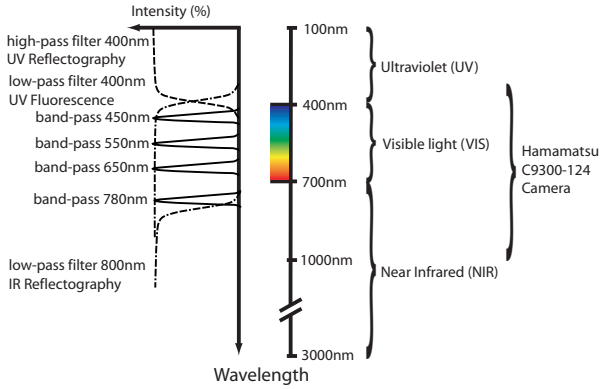


Figure 1: The electromagnetic spectrum and filter response on our acquisition setup.

| No. | Filter type | Illumination |
|---|---|---|
| 1 | SP 400 | UV |
| 2 | LP 400 | UV |
| 3 | LP 400 | VIS-NIR |
| 4 | BP 450 | VIS-NIR |
| 5 | BP 550 | VIS-NIR |
| 6 | BP 650 | VIS-NIR |
| 7 | BP 780 | VIS-NIR |
| 8 | LP 800 | IR |
| 9 | none | VIS-NIR |

Table 1: Description of the MSI containing filter type and the methodology of image acquisition. LP is a long pass filter, SP a short pass filter and BP is a band pass filter.

Selected MSI can be seen in Figure 2. It shows that the IR images have low contrast. Better contrast is obtained in the UV and blue range of the spectrum. Concerning the writing material only iron gall inks of various chemical compositions could be determined on the parchment folios [12].

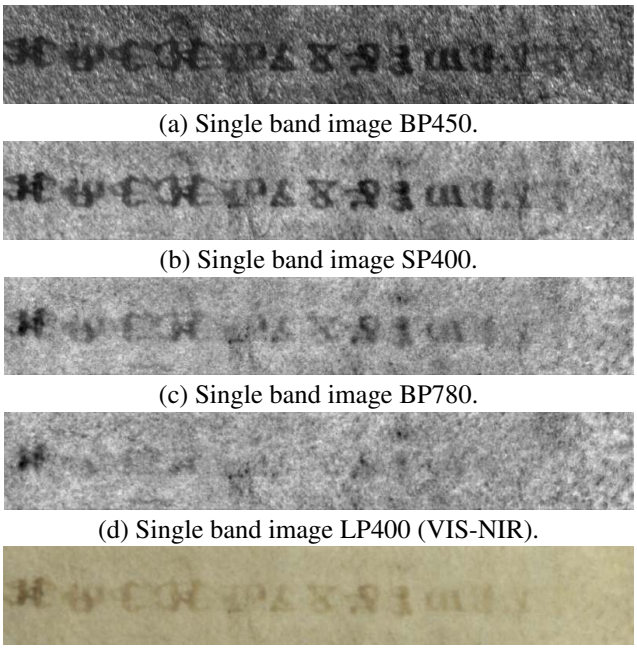

(a) Single band image BP450.

(b) Single band image SP400.

(c) Single band image BP780.

(d) Single band image LP400 (VIS-NIR).

(e) RGB color Image (Nikon).

Figure 2: Selected MSI from folio 29 *recto*.

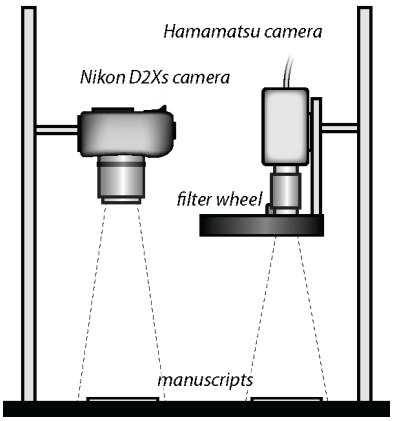


Figure 3: Acquisition setup.

## 3. PREPROCESSING

Distortions of the document images vary the probability densities for the foreground and the background. Therefore, we use background light normalization to avoid these distortions. The method was proposed by Shi and Govindaraju [17] and presents a good normalization approach especially for historical document images. The algorithm uses an adaptive linear function which approximates the uneven background of the images. This uneven background is caused by an uneven illumination during the capturing of the images, or by the aging process of the manuscript pages. After the calculation of the linear function, the images are normalized with respect to the approximation.

## 4. MARKOV RANDOM FIELD MODEL FOR CHARACTER SEGMENTATION

The MSI is defined over a finite rectangular lattice $\mathscr{S} = \{s_1, s_2, \ldots, s_n\}$ in which $1 \ldots n$ indicates the pixel index and the observations $\vec{f}_s \in \mathscr{F}$ for each pixel $s$ represent the multispectral feature vectors used for partitioning the image. The goal is to find a labeling $\omega \in \Omega$ which separates the characters or text pixels from the background. Given a set of feature vectors $\mathscr{F}$ and the set $\Omega$ of all possible segmentations our purpose is to find the segmentation $\hat{\omega}$ with the highest probability. A widely accepted standard is to construct this probability measure within a Bayesian framework [8]:

$$\Pr(\omega|\mathscr{F}) \propto \Pr(\mathscr{F}|\omega)\Pr(\omega), \tag{1}$$

where $\Pr(\omega)$ depicts the prior probability and $\Pr(\mathscr{F}|\omega)$ is the likelihood. $\hat{\omega}$ which maximizes the posterior probability $\Pr(\omega|\mathscr{F})$ can be found via the the *Maximum A Posteriori* (MAP) estimate [7]:

$$\hat{\omega} = \arg\max \Pr(\mathscr{F}|\omega)P(\omega). \tag{2}$$

### 4.1 Prior Model $\Pr(\omega)$

The prior $\Pr(\omega)$ represents the fact that the segmentation is locally homogeneous [8]. According to the *Hammersly-Clifford theorem* [7], a random field is a MRF if $\Pr(\omega)$ follows a Gibbs distribution

$$\Pr(\omega) = \frac{1}{Z}\exp(-U(\omega)) = \frac{1}{Z}\exp\left(-\sum_{c\in\mathscr{C}} V_C(\omega_c)\right), \tag{3}$$

where $Z = \sum_{\omega\in\Omega}\exp(-U(\omega))$ is a normalizing constant and $U(\omega) = \sum_{c\in\mathscr{C}} V_C(\omega_c)$ is an energy function. $c$ is a set of pixels within a neighbor set $\mathscr{N}$, called *clique*, and $V_c$ denotes the potential function or clique potential of clique $c \in \mathscr{C}$ having the label configuration $\omega_c$.

For a regular lattice $\mathscr{S}$, the neighbor set $\mathscr{N}$ of $i$ is defined as the set of nearby sites within a radius $r$

$$\mathscr{N}_i = \{i' \in \mathscr{S} \,|\, [dist(s_{i'}, s_j)]^2 \leq r, i \neq j\} \tag{4}$$

where $dist(s_{i'}, s_j)$ denotes the Euclidean distance between two pixels $s_{i'}$ and $s_j$. A first order MRF involves only the 4 directly connected pixels, as shown in Figure 4a. The numbers $n = 1 \ldots 5$ indicate the neighboring sites in a $n$-th order neighborhood system [11].

We propose to use stroke properties to cover the spatial dependencies of the characters. Thus $\mathscr{C}$ is the set of all pixels $s$ within a radius $r$, where $r$ corresponds to the mean stroke width. The mean stroke width follows the set of all foreground pixels $S$ and the set of all border pixels $D$ from characters and is computed as $w = 2\frac{N_S}{N_D}$ where $N_S$ and $N_D$ are the number of pixels in $S$ and $D$ [13]. Our experiments for manually segmented characters devoted a mean stroke width of 5 pixels. Thus the prior considers a neighborhood set of at least 4th order. To illustrate the neighborhood system on our images consider Figure 4b. It shows one character from our data set with an white circle corresponding to a neighborhood system of 4th order.

The clique potentials favor similar classes within a neighborhood $\mathscr{N}$

$$V_C = \delta(\omega_s, \omega_r) = \begin{cases} +1 & \text{if } \omega_s \neq \omega_r \\ -1 & \text{otherwise} \end{cases} \tag{5}$$

Thus, the full prior is given as follows:

$$\Pr(\omega) = \frac{1}{Z}\exp\left(-\sum_{\{s,r\}\in\mathscr{C}} \delta(\omega_s, \omega_r)\right) \tag{6}$$

| | | | | |
|---|---|---|---|---|
| 5 | 4 | 3 | 4 | 5 |
| 4 | 2 | 1 | 2 | 4 |
| 3 | 1 | x | 1 | 3 |
| 4 | 2 | 1 | 2 | 4 |
| 5 | 4 | 3 | 4 | 5 |

(a)

(b)

Figure 4: (a) Neighborhood system [11] and (b) a character with marked neighborhood system of 4th order.

### 4.2 Observation Model $\Pr(\mathscr{F}|\omega)$

The observation model or image process $\mathscr{F}$ can be formalized as follows: $\Pr(\mathscr{F}|\omega)$ follows a normal distribution $N(\mu, \Sigma)$ [8]. Each class $\omega_t$ and $\omega_b$ (text and background) is represented by its mean vector $\mu_\omega$ and covariance matrix $\Sigma_\omega$ by $\mathscr{N}(\mu_\omega, \Sigma_\omega)$:

$$\frac{1}{\sqrt{(2\pi)^n |\Sigma_\omega|}}\exp\left(-\frac{1}{2}\left(\vec{f} - \vec{\mu_\omega}\right)\Sigma_\omega^{-1}\left(\vec{f} - \vec{\mu_\omega}\right)^T\right), \tag{7}$$

$n$ is the dimension of the MSI. The entities are modeled by a Gaussian mixture model (GMM). Given a GMM, the goal is to maximize the likelihood function with respect to the parameters $\mu$ and $\Sigma$. An elegant and powerful method for finding maximum likelihood solutions for models with latent variables is the *Expectation-Maximization* (EM) algorithm [8, 5]. Applying EM on the MSI we obtain $\mu_t$ and $\Sigma_t$ for the characters as well as $\mu_b$ and $\Sigma_b$ for the background.

### 4.3 Posterior Energy $P(\omega|\mathscr{F})$

According to [8] the posterior probability can be simplified by including the contribution of the likelihood term via the singletons (i.e. pixel sites $s \in \mathscr{S}$)

$$\Pr(\omega|\mathscr{F}) \propto \exp(-U(\omega, \mathscr{F}))$$
$$\propto \exp\left(-\left(\sum_{s\in\mathscr{S}} V_s(\omega_s, \vec{f}_s) + \beta \sum_{\{s,r\in\mathscr{C}\}} \delta(\omega_s, \omega_r)\right)\right)$$

where $\beta > 0$ is a weighting parameter controlling the prior, i.e. the influence of the neighborhood connectivity. The singleton potentials $V_s(\omega_s, \vec{f}_s)$ of pixel sites $s$ are obtained from Eq. 7 by $V_s(\omega_s, \vec{f}_s)$ which equals

$$\ln(\sqrt{(2\pi)^n|\Sigma_{\omega s}|}) + \frac{1}{2}(\vec{f}_s - \vec{\mu}_{\omega_s})\Sigma_{\omega_s}^{-1}(\vec{f}_s - \vec{\mu}_{\omega_s})' \tag{8}$$

The energy function $U(\omega, \mathscr{F})$ of the MRF image segmentation model has the following form:

$$\sum_{s\in\mathscr{S}}\left(\ln(\sqrt{(2\pi)^n|\Sigma_{\omega s}|}) + \frac{1}{2}(\vec{f}_s - \vec{\mu}_{\omega_s})\Sigma_{\omega_s}^{-1}(\vec{f}_s - \vec{\mu}_{\omega_s})'\right)$$
$$+\beta \sum_{\{s,r\in\mathscr{C}\}} \delta(\omega_s, \omega_r)$$

It is clear that Eq. 2 is equivalent to the following energy minimization problem:

$$\hat{\omega} = \arg\min U(\omega, \mathscr{F}) \tag{9}$$

Energy optimization in finding MAP-MRF solutions can be done by either local methods, like Iterated Conditional Modes (ICM) [1], or global methods like simulated annealing [11]. We use ICM to solve this global energy which are a good tradeoff between quality and computing time [8]. ICM uses a deterministic strategy to find local minimums. It starts with an estimate and then selects a label for each pixel which gives the largest decrease of the energy function. The process is repeated until it converges.

## 5. EXPERIMENTS AND RESULTS

The proposed segmentation method has been tested on a varied set of MSI of ancient documents. The test set consists of MSI of 3 folios (17 *recto*, 29 *recto* and 30 *verso*) for which we generated the ground truth (GT) data by manually segmenting the characters. This step was supported by philologists which are experts in analyzing the documents given. Figure 5 shows details from folio 29 *recto* including a single band of the MSI with highest contrast (BP450) (a) and the corresponding GT data in (b).

We compared our method to character segmentation approaches developed especially for ancient, low contrast or noisy document images. The serialization of the *k*means algorithm by Leydier et al. [10] is the first method and the Sauvola binarization method [16] which is performed on the BP450 single band image constitutes the second method. We use the *precision* and *recall* rate to measure the accuracy metric and to rank the performance of the different methods:

$$\textit{precision} = \frac{\#\text{ of text pixels correctly classified}}{\#\text{ of text pixels detected}} \tag{10}$$

$$\textit{recall} = \frac{\#\text{ of text pixels correctly classified}}{\#\text{ of text pixels in GT}} \tag{11}$$

| $\beta = 0.1$ | $n=1$ | $n=2$ | $n=3$ | $n=4$ | $n=5$ |
|---|---|---|---|---|---|
| precision | 0.81 | 0.81 | 0.82 | 0.82 | 0.80 |
| recall | 0.62 | 0.65 | 0.65 | 0.78 | 0.70 |
| $\beta = 0.3$ | $n=1$ | $n=2$ | $n=3$ | $n=4$ | $n=5$ |
| precision | 0.80 | 0.79 | 0.83 | 0.79 | 0.75 |
| recall | 0.67 | 0.73 | 0.66 | 0.80 | 0.66 |

Table 2: Evaluation of neighborhood of *n*th order and $\beta$.

The first experiment aimed to analyze the behavior of the neighborhood system $\mathscr{N}$ and the weighting parameter $\beta$. We compared different orders $n$ of MRF along them a first order MRF which is used for instance in [8, 3]. Table 2 shows the *precision* and *recall* rate for $\beta = 0.1$ and $\beta = 0.3$ and a neighborhood system $n = 1 \ldots 5$. It can be seen that the *recall* values are very low for $n = 1 \ldots 3$ which reason is the background noise. The best solution is obtained with $n = 4$ and $\beta = 0.1$ which is in concordance to the proposed stroke characteristics. Generally it can be said that the smaller the considered neighborhood system, the more noise emerges in the background. On the other side, a neighborhood set considering to much pixels leads to missing characters or to closed character gaps or holes. The influence of $\beta$ is likewise. The smaller $\beta$ the more noise we have and values chosen too big cause missing characters ($\beta \geq 5$).

Compared to *k*means clustering and the Sauvola binarization technique the proposed method showed the best results. Figure 5 shows details from folio 29 *recto* after the segmentation with the Sauvola binarization method (c), *k*means clustering (d), and the MRF approach (e) with parameters $\beta = 0.1$ and a neighborhood of 4th order. It can be seen that especially the thresholding image contains a lot of noise in the background and even within the characters. The *k*means method performs better but the rightmost character was not segmented and others are broken. The result of the MRF approach segments even the rightmost character which has very low contrast and is even hard to detect by experts. The *precision* and *recall* rate for the evaluation with the GT data can be seen in Table 3. For folio 17 *recto* and 30 *verso* the *k*means shows suboptimal results due to low contrast. The locally performing thresholding method shows better results but has low *precision*. The MRF method has the best performance with a mean *precision* rate of 0.88 and a mean *recall* rate of 0.70.

(a) Single band image BP450.

(b) GT data.

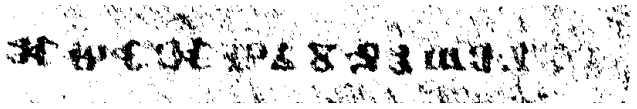

(c) Output of the Sauvola algorithm.

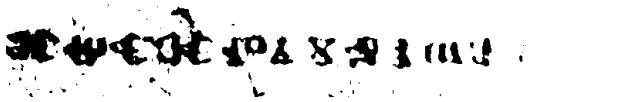

(d) Output of the *k*means algorithm.

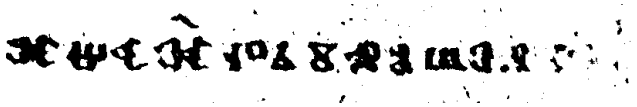

(e) Output of the proposed MRF algorithm.

Figure 5: Detail from folio 29 *recto*: BP450, GT data, and comparison of results.

| Folio | | *k*means | MRF | Sauvola |
|---|---|---|---|---|
| 17 *recto* | precision | 0.58 | 0.93 | 0.67 |
| | recall | 0.34 | 0.64 | 0.72 |
| 29 *recto* | precision | 0.67 | 0.82 | 0.63 |
| | recall | 0.72 | 0.78 | 0.61 |
| 30 *verso* | precision | 0.54 | 0.90 | 0.73 |
| | recall | 0.75 | 0.68 | 0.72 |
| Average | precision | 0.59 | 0.88 | 0.68 |
| | recall | 0.60 | 0.70 | 0.68 |

Table 3: Precision and Recall.

## 6. CONCLUSIONS AND OUTLOOK

This paper demonstrated the effectiveness of combining spatial and spectral features for character segmentation in MSI of ancient manuscripts. The method is based on a MRF model and we use stroke characteristics to incorporate contextual spatial information. Compared to methods like thresholding or clustering of spectral features the proposed algorithm was even able to detect low contrast characters where other methods failed. Furthermore, due to the consideration of spatial context we obtain lower noise within the background and within the text regions.

Indeed dark stained areas within the folios affect the segmentation. Such stains are detected as foreground, even when there is enough contrast to read the characters. A solution is to remove these areas before learning the observation model. Further future work includes the usage of recently proposed energy minimization algorithms like graph cuts to improve the performance of the energy minimization [18]. Then a detailed evaluation of the results will be also based on OCR and a quality validation by experts. Furthermore we will test extensive the multispectral nature of the measurements and compare several permutations.

## 7. ACKNOWLEDGMENT

This work was supported by the Austrian Science Fund (FWF) under grant P19608-G12.

## REFERENCES

[1] J. Besag. On the statistical analysis of dirty pictures. *Journal of the Royal Statistical Society*, 48(3):259–302, 1986.

[2] J. Brauers, N. Schulte, and T. Aach. Multispectral Filter-Wheel Cameras: Geometric Distortion Model and Compensation Algorithms. *IEEE Trans. on Image Processing*, 17(2):2368–2380, December 2008.

[3] H. Cao and V. Govindaraju. Handwritten carbon form preprocessing based on markov random field. In *Intl. Conference on Computer Vision and Pattern Recognition (CVPR 2007)*, Minneapolis, Minnesota, USA, 2007.

[4] M. Diem, M. Lettner, and R. Sablatnig. Registration of multi-spectral manuscript images. In *8th International Symposium on Virtual Reality, Archaeology and Cultural Heritage*, pages 133–140, Brighton, UK, 2007.

[5] R. Duda, P. Hart, and D. Stork. *Pattern Classification*. Wiley-Interscience, New York, 2nd edition, 2001.

[6] R. Easton, K. Knox, and W. Christens-Barry. Multispectral Imaging of the Archimedes Palimpsest. In *32nd Applied Image Pattern Recognition Workshop, AIPR 2003*, pages 111–118, Washington, DC, October 2003.

[7] S. Geman and D. Geman. Stochastic relaxation, gibbs distributions and the bayesian restoration of images. *IEEE Trans. Pattern Anal. Mach. Intell.*, 6(6):721–741, November 1984.

[8] Z. Kato and T.-C. Pong. A markov random field image segmentation model for color textured images. *Image and Vision Computing*, 24:1103–1114, 2006.

[9] M. Lettner, F. Kleber, R. Sablatnig, and H. Miklas. Contrast Enhancement in Multispectral Images by Emphasizing Text Region. In *8th IAPR International Workshop on Document Analysis Systems*, pages 225–232, Nara, Japan, September 2008.

[10] Y. Leydier, F. L. Bourgeois, and H. Emptoz. Serialized unsupervised classifier for adaptative color image segmentation: Application to digitized ancient manuscripts. In *17th International Conference on Pattern Recognition*, pages 494–497, Cambridge, UK, 2004.

[11] S. Li. *Markov Random Field Modeling in Computer Vision*. Springer, 1995.

[12] H. Miklas, M. Gau, F. Kleber, M. Lettner, M. Vill, R. Sablatnig, M. Schreiner, M. Melcher, and G. Hammerschmid. St. Catherine' s Monastery on Mount Sinai and the Balkan-Slavic Manuscript-Tradition. In H. Miklas and A. Miltenova, editors, *Slovo: Towards a Digital Library of South Slavic Manuscripts*, pages 13–36, 2008.

[13] V. Pervouchine, G. Leedham, and K. Melikhov. Handwritten character skeletonisation for forensic document analysis. In *Proc. ACM Symposium on Applied Computing (SAC)*, pages 754–758, Santa Fe, New Mexico, USA, 2005.

[14] K. Rapantzikos and C. Balas. Hyperspectral Imaging: Potential in Non-Destructive Analysis of Palimpsests. In *IEEE International Conference on Image Processing*, volume 2, pages 618–621, 2005.

[15] E. Salerno, A. Tonazzini, and L. Bedini. Digital image analysis to enhance underwritten text in the Archimedes palimpsest. *International Journal on Document Analysis and Recognition*, 9(2-4):79–87, 2007.

[16] J. Sauvola and M. Pietikainen. Adaptive document image binarization. *Pattern Recognition*, 33(2):225–236, 2000.

[17] Z. Shi and V. Govindaraju. Historical document image enhancement using background light intensity normalization. In *17th International Conference on Pattern Recognition*, pages 473–476, Washington, DC, USA, 2004.

[18] R. Szeliski, R. Zabih, D. Scharstein, O. Veksler, V. Kolmogorov, A. Agarwala, M. Tappen, and C. Rother. A comparative study of energy minimization methods for markov random fields with smoothness-based priors. *IEEE Trans. Pattern Anal. Mach. Intell.*, 30(6):1068–1080, 2008.

[19] C. M. Thillou and B. Gosselin. Spatial and color spaces combination for natural scene text extraction. In *Int. Conference on Image Processing ICIP06*, pages 985–988, October 2006.

[20] K. Wang, J. A. Kangas, and W. Li. Character segmentation of color images from digital camera. In *6th International Conference on Document Analysis and Recognition (ICDAR01)*, pages 210–214, Washington, DC, USA, September 2001.

[21] C. Wolf and D. S. Doermann. Binarization of low quality text using a markov random field model. In *Proceedings of the International Conference on Pattern Recognition (ICPR02)*, Quebec, Canada, August 2002.